International Immunopharmacology 128 (2024) 111535

Contents lists available at ScienceDirect

International Immunopharmacology

journal homepage: www.elsevier.com/locate/intimp

ACE2 improves endothelial cell function and reduces acute lung injury by downregulating FAK expression

Yixuan He [a], Baocai Gang [a], Mengjie Zhang [a], Yuting Bai [a], Ziyu Wan [a], Jiesong Pan [a], Jie Liu [b], Guoquan Liu [a,*], Wei Gu [a,*]

[a] Department of Biochemistry and Molecular Biology, School of Laboratory Medicine, and Anhui Province Key Laboratory of Cancer Translational Medicine, Bengbu Medical University, 2600 Donghai Avenue, Bengbu, Anhui Province 233030, PR China
[b] College of Animal and Veterinary Sciences, Southwest Minzu University, Chengdu, Sichuan Province, PR China

ARTICLE INFO

Keywords:
ACE2
FAK
ANG1-7
Endothelial cells
Acute lung injury

ABSTRACT

Endothelial cell (EC) barrier dysfunction and increased adhesion of immune inflammatory cells to ECs crucially contribute to acute lung injury (ALI). Angiotensin-converting enzyme 2 (ACE2) is an essential regulator of the renin-angiotensin system (RAS) and exerts characteristic vasodilatory and anti-inflammatory effects. SARS-COV-2 infects the lungs by binding to ACE2, which can lead to dysregulation of ACE2 expression, further leading to ALI with predominantly vascular inflammation and eventually to more severe acute respiratory distress syndrome (ARDS). Therefore, restoration of ACE2 expression represents a valuable therapeutic approach for SARS-COV-2-related ALI/ARDS. In this study, we used polyinosinic-polycytidylic acid (Poly(I:C)), a double-stranded RNA analog, to construct a mouse ALI model that mimics virus infection. After Poly(I:C) exposure, ACE2 was downregulated in mouse lung tissues and in cultured ECs. Treatment with DIZE, an ACE2-activating compound, upregulated ACE2 expression and relieved ALI in mice. DIZE also improved barrier function and reduced the number of THP-1 monocytes adhering to cultured ECs. Focal adhesion kinase (FAK) and phosphorylated FAK (p-FAK) levels were increased in lung tissues of ALI mice as well as in Poly(I:C)-treated ECs in vitro. Both DIZE and the FAK inhibitor PF562271 decreased FAK/p-FAK expression in both ALI models, attenuating ALI severity in vivo and increasing barrier function and reducing monocyte adhesion in cultured ECs. Furthermore, in vivo experiments using ANG 1–7 and the MAS inhibitor A779 corroborated that DIZE-mediated ACE2 activation stimulated the activity of the ANG 1–7/MAS axis, which inhibited FAK/p-FAK expression in the mouse lung. These findings provide further evidence that activation of ACE2 in ECs may be a valuable therapeutic strategy for ALI.

1. Introduction

Acute lung injury (ALI) is a clinical syndrome characterized by hypoxemia, respiratory distress, and noncardiogenic pulmonary edema [1]. The key pathological cause of ALI is pulmonary endothelial cell (EC) dysfunction [2,3]. In ALI, an excessive inflammatory response promotes EC activation and recruitment and infiltration of inflammatory cells, such as neutrophils and monocytes, leading to disruption of the endothelial barrier function [4,5]. It has been shown that SARS-COV-2 causes ALI, which may worsen to acute respiratory distress syndrome (ARDS), by triggering vascular EC dysfunction leading to immune cell adhesion, thrombosis, uncontrolled production of pro-inflammatory factors (cytokine storm), vascular hyperpermeability, and ultimately overt vasculopathy that exacerbates ALI symptoms [6,7]. Therefore, targeting ECs to prevent the adhesion and infiltration of immune inflammatory cells and to restore barrier integrity represents a strong strategy for developing ALI therapies. Poly(I:C) is a synthetic double-stranded RNA analog that is commonly used to mimic viral infections. It stimulates interferon (IFN) expression, thus exerting antiviral effects, and it also induces an over-immune response to promote inflammation and it is experimentally used to study virus-associated inflammatory responses [8,9]. Numerous studies demonstrated that Poly(I:C) induces virus-like inflammation in neural, liver, and lung/airway tissues [10–13]. In our laboratory, we have successfully constructed a mouse ALI model using

* Corresponding authors at: Department of Biochemistry and Molecular Biology, School of Laboratory Medicine, Bengbu Medical University, 2600 Donghai Street, Bengbu, 233030 Anhui Province, PR China.
E-mail addresses: guoquanliu@bbmc.edu.cn (G. Liu), guwei@bbmc.edu.cn (W. Gu).

https://doi.org/10.1016/j.intimp.2024.111535
Received 16 November 2023; Received in revised form 1 January 2024; Accepted 10 January 2024

Table 1
Sequence of si-RNA.

Product code	Product name	Product sequence
stB0000153A	genOFFTM st-h-MAS1_001	AGAGTCACTCTCGGAATGA
stB0000153B	genOFFTM st-h-MAS1_002	AGTAGCGCCAACCCTTTCA

Poly(I:C) [14].

ACE2, a homologue of the angiotensin-converting enzyme (ACE), is widely expressed in many cells and tissues, including ECs [15]. ACE2 exerts multiple cellular functions and affects the balance of the renin-angiotensin system (RAS) by converting angiotensin II (ANG II) to angiotensin 1–7 (ANG 1–7) [16]. Unlike ANG II, ANG 1–7 has vasodilatory, anti-fibrotic, and anti-inflammatory actions, and disrupted ACE2 expression is associated with inflammatory and fibrotic responses in tissues and cells [17,18]. Notably, ACE2 acts also as an essential receptor for SARS-COV-2 infection. At the early stage, the latter promotes an increase in ACE2 expression on the surface of human airway epithelial cells, which facilitates systemic dissemination of the virus through the respiratory tract [19]. However, as the infection progresses, cell surface ACE2 expression is decreased via internalization and shedding mediated by activation of a disintegrin and metalloproteinase 17 (ADAM17) [20]. Studies have shown that SARS-COV-2 triggers also vascular EC injury upon binding to ACE2 proteins on the EC surface, which decreases ACE2 expression [21]. Moreover, ACE2 expression and enzymatic activity are ultimately reduced in ALI; this leads to dysregulation of the local RAS environment, with disruptive effects on EC function [20,22].

Diminazene aceturate (DIZE) and MLN-4760 are synthetic small molecule drugs that specifically promote and inhibit, respectively, ACE2 protein expression. DIZE was shown to exert protective effects in animal models of hypertension and myocardial infarction [23,24]. Although direct experimental evidence is still lacking, DIZE has been also suggested as a candidate drug for the treatment of complications due to SARS-COV-2 infection [25]. Therefore, investigating the effects of DIZE-mediated upregulation of ACE2 on ALI-related EC dysfunction may provide a new therapeutic strategy to treat SARS-COV-2-induced ALI/ARDS.

Focal adhesion kinase (FAK) is a tyrosine protein kinase involved in the regulation of cell growth, cell migration, and epithelial/endothelial barrier function [26–29]. In melanoma and gastric cancer models, increased FAK expression promotes tumor cell migration and proliferation [30,31]. During TNF-α-induced inflammation of ECs, FAK binds to paxillin and promotes neutrophil migration across the endothelium and toward the lesion, which can be blocked by inhibiting either FAK or paxillin [32]. FAK and its phosphorylated form (p-FAK) are both increased during reactive oxygen species (ROS)-induced disruption of EC barrier function [33]. Several potent and specific small molecule FAK inhibitors have been developed, with a large body of evidence suggesting that they can inhibit the proliferation and migration of tumor cells [34,35]. PF562271 is a safe, potent, and specific FAK inhibitor; it is therefore of interest to explore whether PF562271 can be used to treat ALI-related EC dysfunction [36]. ACE2 directly binds to integrins, the upstream activators of FAK, to regulate FAK expression [37]. Thus, the regulation of the RAS by ACE2 is closely related to modulation of FAK expression/activity. ANG II promotes FAK/p-FAK expression during the pathogenesis of intestinal and cardiovascular diseases [38–40]. Since ACE2 hydrolyzes ANG II to generate ANG 1–7, it is hypothesized that ACE2 activity would have a suppressing effect on FAK. However, whether ACE2 can inhibit the expression and phosphorylation of FAK in animal and EC models of ALI remains to be proved.

In the present study, we used a mouse model of Poly(I:C)-induced ALI and Poly(I:C)-treated human ECs to investigate whether the ACE2 activator DIZE can ameliorate ALI, improve EC barrier function, and reduce inflammatory immune cell adhesion to ECs. In addition, the regulatory effects of the ACE2 inhibitor MLN-4760 and the FAK inhibitor PF562271 on the ANG1-7-MAS axis and on FAK/p-FAK expression were assessed in both experimental models. Our findings suggest that pharmacological activation of ACE2 in combination with FAK suppression may be a valid therapeutic strategy to treat ALI/ARDS.

Table 2
Sequence of primer for RT-PCR.

Gene	Forword primer (5′-3′)	Reverse primer (5′-3′)
GAPDH	CCACCTTCGATGCCGGGGCTG	GGCTCCCTAGGCCCCTCCTGTT
TNF-α	AAAAGCAAGCAGCCAACCAG	AGTGCCTCTTCTGCCAGTTC
IL-6	TCTATACCACTTCACAAGTCGGA	GAATTGCCATTGCACAACTCTTT
IL-8	GGAATTTCCACCGGCAATGA	CTGCCTGTCAAGCTGACTTC

2. Materials and methods

2.1. Experimental animals

C57BL/6 mice (SKbex Biotech, Henan, China) weighing 18–25 g and aged 7–8 weeks were used in this study. Mouse airway injection of Polyinosinic: polycytidylic acid (Poly(I:C); APExBIO, Houston, TX, USA) was used to construct an ALI model. To this end, mice were anesthetized, the trachea was incised, and Poly(I:C) (2.5 mg/kg) was injected for 6 h. PF562271 (10 mg/kg; Beyotime, Shanghai, China), ANG 1–7 (0.06 mg/kg; MedChemExpress, Monmouth Junction, NJ, USA), and A779 (10 μg/kg; MedChemExpress) were injected 24 h prior to Poly(I:C) administration. Diminazene aceturate (DIZE, 15 mg/kg; MedChemExpress) and MLN-4760 (1 mg/kg; MedChemExpress) were injected 12 h prior to Poly (I:C) injection. The number of mice receiving individual drugs or drug combinations was in each case 4 (n = 4 per group). After treatment, mouse lung tissues were collected and processed for downstream assays. This study was performed following the China Council on Animal Care and Protocol guidelines. In addition, the procedures for animal care and use were approved by the Ethics Committee of Bengbu Medical College (2021–003), and all applicable institutional and governmental regulations concerning the ethical use of animals were followed.

2.2. Cell culture and siRNA transfection

Human umbilical vein endothelial cells (HUVECs) and human monocytic leukemia cells (THP-1 cells) were obtained from our laboratory. HUVECs were cultured in high-sucrose DMEM (Gibco, Waltham, MA, USA) containing 10 % FBS (Gibco) at 37 °C and 5 % CO_2. THP-1 cells were cultured in RPMI-1640 medium (Gibco) containing 10 % FBS at 37 °C and 5 % CO_2. Cells were cultured in plates of different sizes. Poly(I:C) (10 μg/ml) was utilized to simulate an ALI environment in vitro for 48 h. DIZE (10 μM) and MLN-4760 (10 μM) were added 12 h after the addition of Poly(I:C). ANG 1–7 (80 nM) and PF562271 (25 μg/ml) were added 24 h after addition of Poly(I:C). Transient si-RNA transfection procedures were performed in HUVECs 6 h prior to incubation with Poly(I:C). Table 1 lists the si-RNA sequences (RiboBio, GuangZhou, China) used for transfection.

2.3. Western blotting

Lung tissue lysates and cultured cell lysates were generated in 1 ml of tissue lysis buffer (RIPA and PMSF, 1:100) (Beyotime) and supernatants obtained by centrifugation (4 °C, 16,543 × g for 5 min) for immunoblotting experiments. The samples were loaded onto SDS-polyacrylamide gels, separated by electrophoresis, and transferred to nitrocellulose membranes. After blocking with skim-milk, primary antibodies specific for ACE2 (221115–1-AP, AB_10732845, Proteintech Group, Rosemont, IL, USA), FAK (66258–1-IG, AB_2881646, Proteintech Group), p-FAK (8556, AB_10891442, Cell Signaling, Boston, MA, USA), ANG 1–7 (MAS085Ge21, CLOUD-CLONE CORP, Houston, TX, USA), MAS (20080–1-AP, AB_10665372, Proteintech Group), GAPDH

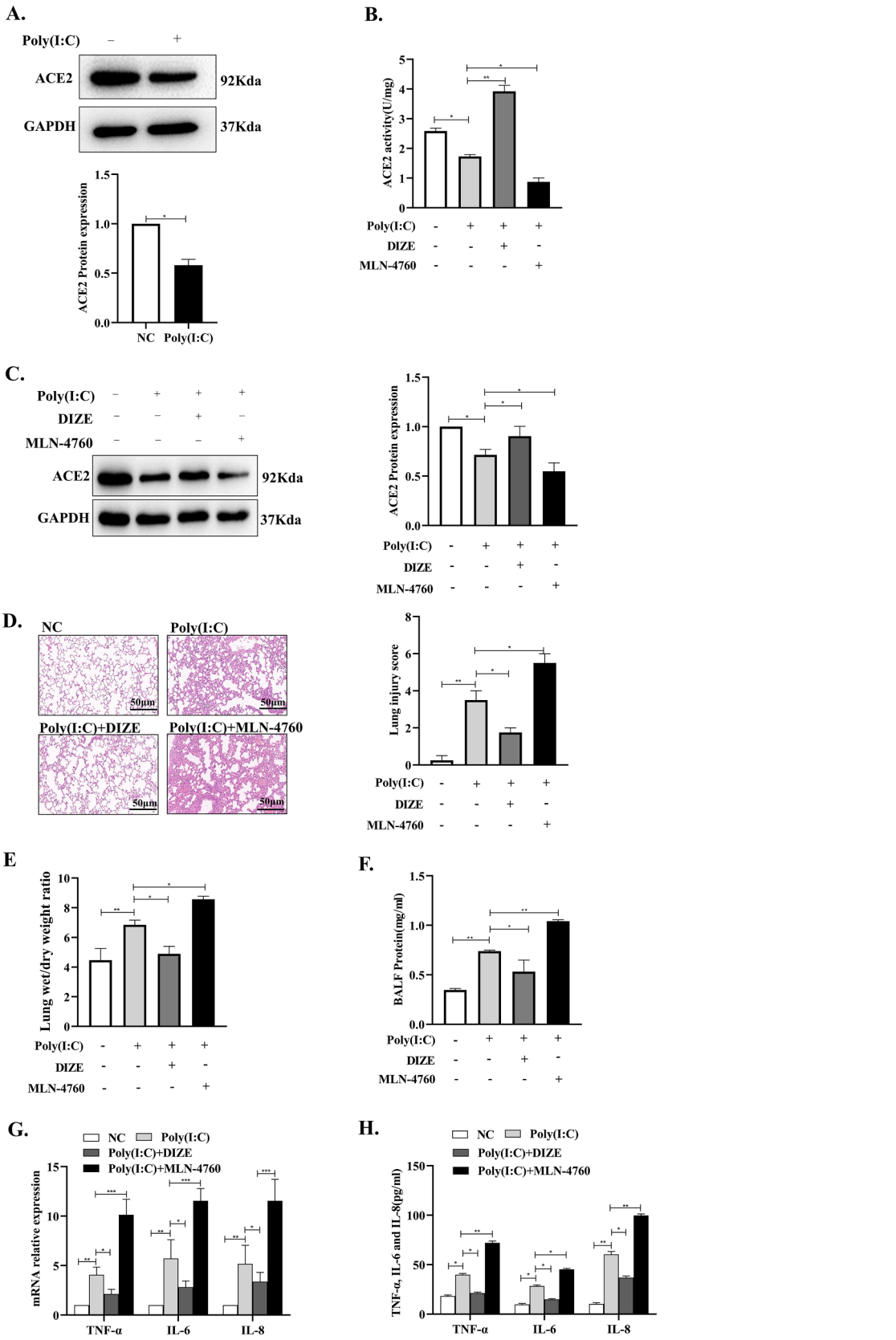

(caption on next page)

Fig. 1. DIZE-induced ACE2 expression alleviates ALI in Poly(I:C)-treated mice. (A) Western blot analysis of ACE2 expression in the lungs of vehicle-treated control (NC) and Poly(I:C)-treated (ALI) mice (n = 8 per group). (B) ACE2 Enzymatic Activity changes in lung tissues of Poly(I:C)-treated mice treated with DIZE and MLN-4760 (n = 4 per group). (C) Western blot analysis of ACE2 expression in lung tissues of Poly(I:C)-treated (ALI) mice treated with DIZE and MLN-4760 (n = 4 per group). (D) Histopathological changes and lung injury scores in DIZE- and MLN-4760-treated mice. (E, F) Lung wet/dry weight ratio estimations and BALF total protein concentration changes in DIZE- and MLN-4760-treated mice. (G) Analysis of TNF-α, IL-6, and IL-8 mRNA expression in lung tissues from DIZE- and MLN-4760-treated ALI mice (n = 4 per group). (H) ELISA was used to detect the levels of TNF-α, IL-6, and IL-8 expression in lung tissues of Poly(I:C)-treated mice treated with DIZE and MLN-4760 (n = 4 per group). $^{*}P < 0.05$; $^{**}P < 0.01$; $^{***}P < 0.001$.

(60004–1-Ig, AB_2107436, Proteintech Group), and α-TUBULIN (66031–1-Ig, AB_11042766, Proteintech Group) were added overnight at 4 °C. This was followed by incubation with horseradish peroxidase (HRP)-coupled sheep anti-mouse or rabbit secondary antibodies at room temperature for 2 h. Finally, ECL images were taken after signal development using a BeyoECL Moon Kit (Beyotime). Protein band density detection was performed using ImageJ software.

2.4. Lung histopathology

Lung tissues were collected and fixed in 5 % paraformaldehyde, cut into 5-μm-thick sections, stained with hematoxylin and eosin, and visualized by light microscopy. Scoring of histopathological findings was performed using the ATS standard.

2.5. Lung wet/dry weight ratio

After euthanasia, mouse lungs were rapidly excised and their weight recorded as wet weight. The lungs were dried at 60 °C for 72 h, after which dry weights were recorded for estimations of lung wet/dry weight ratios.

2.6. Collection of bronchoalveolar lavage fluid (BALF) and total protein analysis

Following thoracotomy, the mouse trachea was cut open and the BALF was collected by repeatedly rinsing the lungs with PBS. The samples were centrifuged at 1000*g* for 10 min at 4 °C and the supernatants and precipitates collected. Total protein concentration in BALF samples was determined with a BCA kit (Beyotime).

2.7. RNA isolation and quantitative RT-PCR

Lung tissues or cells were lysed with total RNA Isolation Reagent (Biosharp, Hefei, China) and corresponding total RNA contents isolated by chloroform extraction and isopropanol-ethanol precipitation. The RNA was reverse-transcribed into cDNA using a BeyoRT™ II cDNA First Strand Synthesis Kit (Beyotime). cDNA samples were subjected to real-time PCR amplification using ChamQ Universal SYBR Master Mix reagent (Vazyme, Nanjing, China), which was configured using qPCR Master Mix (Vazyme). The expression of target genes (Table 2) was normalized to that of control samples, and fold change expression was calculated using the $2^{-\Delta\Delta}C_t$ method, with GAPDH as an internal control. All experiments were performed in triplicate.

2.8. Cell viability assay

HUVECs were collected during the logarithmic growth phase and seeded into 96-well plates at a density of 2×10^4 cells/well (200 μl of cell suspension per well). Cells were incubated in a 37 °C/5% CO_2 incubator. After adhesion to the dish surface, cells were treated with 0 (control), 0.1, 1, 10, 25, or 100 μg/mL Poly(I:C). After an additional 24-h incubation, the culture medium was discarded, 20 μl of CCK-8 solution (Beyotime) was added to each well, and absorbance was detected after 30 min of incubation at 37 °C, 5 % CO_2 in a microplate reader. Cell viability = (OD value of experimental group - OD value of blank group)/(OD value of control group - OD value of blank group) × 100 %.

2.9. ACE2 enzymatic activity assay

Activity of ACE2 in cell and lung tissue were measured by ACE2 Activity Fluorometric Assay Kit (Beyotime), which utilizes the ability of an active ACE2 to cleave a synthetic MCA based peptide substrate to release a free fluorophore. HUVEC treated in different groups were treated according to the instructions of the ACE2 Activity Fluorometric Assay Kit and proportionally prepared into a total volume of 98 μl of reaction system. The samples to be tested and different concentrations of standards were added into a black 96-well plate at the same time, and then the fluorescence intensity was detected under the following conditions: the temperature was 37 °C, the excitation wavelength was 325 nm, the emission wavelength was 393 nm, and the data were read every 10 min for a total of 60 min. The standard curve was set according to the fluorescence intensity of different concentrations of standards. ACE2 activity was measured as: ACE2 activity (nmol/min/mg or U/mg) = A × dil/(Vsample × T × C), where A is the amount of MCA generated (calculated by using the standard curve), dil is the dilution degree of the sample, Vsample is the volume of sample, T is the reaction temperature, C is the concentration of the sample.

2.10. Enzyme-Linked immunosorbent assay (ELISA)

TNF-α, IL-6 and IL-8 in the lung tissue homogenate were detected using Mouse TNF-α ELISA kit (RUIXIN BIOTECH, Quanzhou, China), Mouse IL-6 ELISA kit (RUIXIN BIOTECH) and Mouse IL-8 ELISA (MEIMIAN BIO, Shanghai, China) according to manufacturer's instructions.

2.11. Monocyte adhesion assay

HUVECs in the logarithmic growth phase were harvested, inoculated into 12-well plates and 96-well plates, and allowed to grow to 70 %-80 % confluence, and then grouped for treatment. At this time point, THP-1 cells were collected and incubated with 5 μM calcein-AM (Beyotime) at 37 °C/5% CO_2 for 30 min. Labeled THP-1 cells 2×10^4 cells were then added into the HUVEC cultures established as described above. After 15 min, the wells were rinsed three times with PBS to remove non-adherent cells. Photographs were taken using a Zeiss Observer Z1 inverted fluorescence microscope, and the number of THP-1 cells per well counted using Image J. Fluorescence intensity of each well in a 96-well plate was also detected.

2.12. Transendothelial electrical resistance (TEER) assay

The upper chambers of Transwell inserts (BIOFLI, Guangzhou, China) were seeded with 2×10^5 HUVECs/ml (200 μl final volume). The lower chambers contained 600 μl of high-sucrose DMEM. TEER was measured 0, 12, 24, 36, 48, 60, and 72 h after seeding using a Millicell ERS-2 voltohmmeter (Millipore, Billerica, MA, USA). Growth time-TEER curves were plotted, and the plateau period (48–60 h) was selected for drug treatments. TEER = (endothelial cell resistance value - basal resistance value) × Transwell membrane bottom area (0.33 cm^2).

2.13. FITC-dextran permeability assay

For EC permeability assays, 200 μl of a suspension of 2×10^5 HUVECs/ml was added into the upper chambers of Transwell inserts. The lower chambers contained 600 μl of high-sucrose DMEM. Drug

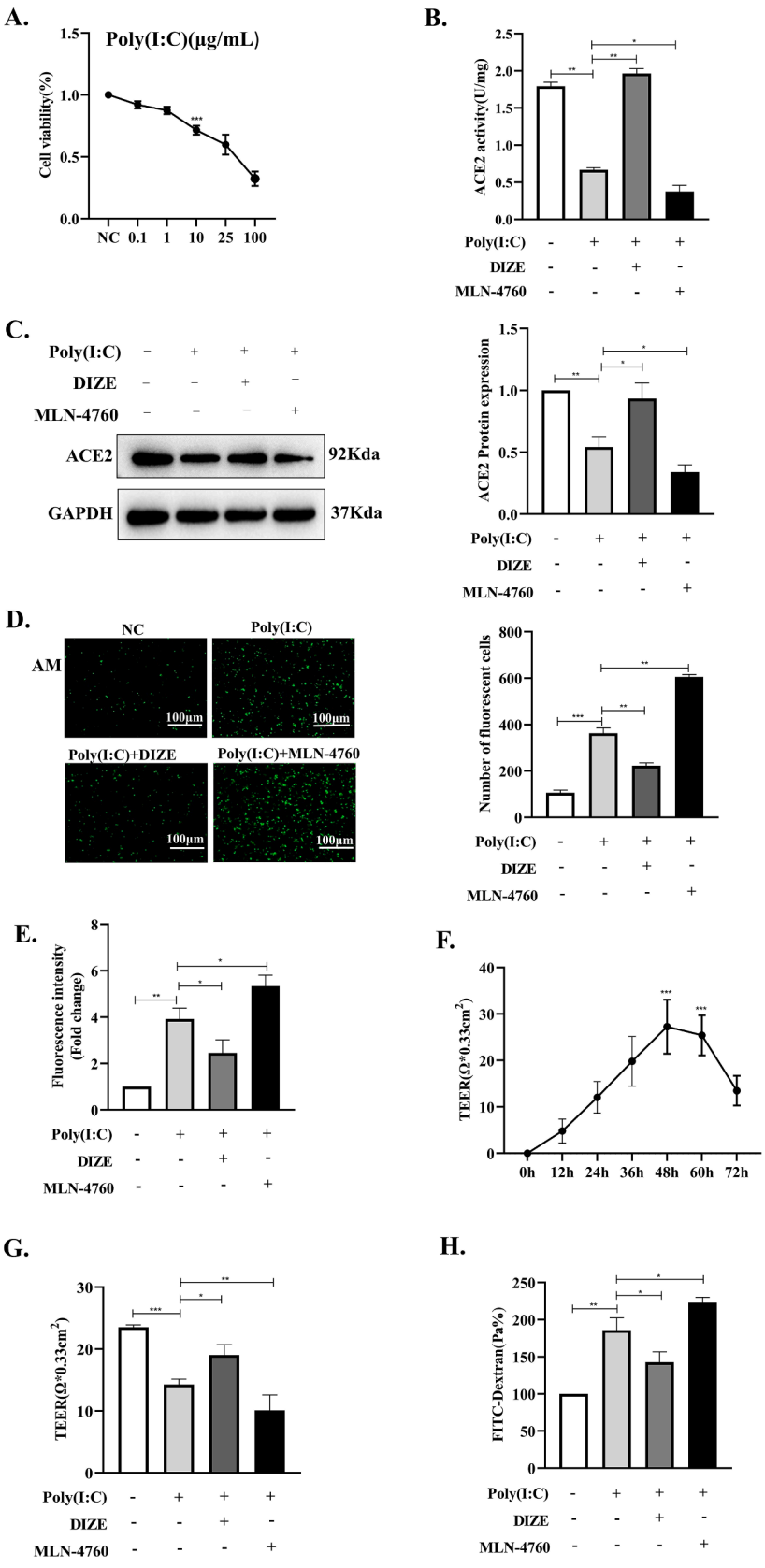

(caption on next page)

Fig. 2. ACE2 upregulation reduces monocyte adhesion and improves barrier function in Poly (I:C)-treated HUVECs. (A) Results of cell viability assays performed in HUVEC treated with different concentrations of Poly(I:C). (B) The effect of DIZE and MLN-4760 on ACE2 Enzymatic Activity changes in Poly(I:C)-treated HUVECs. (C) Western blot analyses examining the effect of DIZE and MLN-4760 on ACE2 expression in Poly(I:C)-treated HUVECs. (D) Results of THP-1 cell adhesion assays in Poly(I:C)-treated HUVEC cultures exposed to DIZE and MLN-4760. (E) Quantification of calcein-AM fluorescence intensity of THP-1 cells that adhered to Poly(I:C)-treated HUVEC exposed to DIZE and MLN-4760. (F) Growth time-TEER curves recorded in cultured HUVECs (*compared with the NC group). (G) TEER values recorded in Poly(I:C)-treated HUVECs exposed to DIZE and MLN-4760. (H) Permeability coefficients of FITC-dextran (Pa%) recorded in cultured HUVECs. $^{*}P < 0.05$; $^{**}P < 0.01$; $^{***}P < 0.001$. N = 3 independent experiments.

treatments were performed on established HUVEC monolayers. After replacing the culture media in the lower chambers with serum-free, high-sucrose DMEM, 0.5 mg/ml FITC-dextran (MedChemExpress) prepared in serum-free, high-sucrose DMEM was added to the upper chambers. After incubation for 1800 sec, media in the upper and lower chamber were independently transferred to a 96-well plate under light-avoidance conditions, and the fluorescence intensity of each well detected in a microplate reader. Permeability was measured as: PA = [A]/t × 1/A × V/[L], where [A] represents the fluorescence value of the lower chamber, t is the incubation time of FITC-dextran (in seconds), A is the filtered area of FITC-dextran (0.33 cm^2), V is the volume of serum-free medium in the lower chamber, and [L] represents the A value of fluorescence in the upper chamber. The results were expressed as Pa% = (Pa value of the test group/Pa value of the control group) × 100 %.

2.14. Statistical analysis

All experiments were performed at least in triplicate, and all values were expressed as means ± SD. Statistical analyses were performed using GraphPad Prism 9.3.0 (GraphPad Software) using one-way ANOVA and Tukey's post-hoc tests for multiple comparisons. $P < 0.05$ was considered significant.

3. Results

3.1. Dize-induced ACE2 expression alleviates ALI in mice

To evaluate the potential role of ACE2 in ALI, we first examined ACE2 expression levels in lung tissue from an ALI mouse model induced by injection of Poly(I:C) [14]. Western blotting results showed that ACE2 protein expression was significantly decreased in inflammatory lung tissues (Fig. 1A). ALI-related ACE2 enzymatic activity decrease and ACE2 downregulation was inhibited after pre-treatment with the ACE2 activator DIZE, and potentiated after pre-treatment with the ACE2 inhibitor MLN-4760 (Fig. 1B and 1C). Suggesting a beneficial role for ACE2 activation in ALI, and consistent with improved lung injury scores, histopathological findings showed that DIZE reduced the number of alveolar cavities, attenuated interstitial congestion and edema, and reduced the thickness of alveolar wall, the infiltration of inflammatory cells and erythrocytes into the alveolar interstitium (Fig. 1D). In contrast, MLN-4760 increased the thickness of alveolar wall, the number of alveolar cavities, exacerbated interstitial congestion and edema, and promoted further infiltration of inflammatory cells and erythrocytes (Fig. 1D). In line with the above findings, DIZE decreased both the lung wet/dry weight ratio and total BALF protein content in ALI mice, whereas further increases in both variables were noted after MLN-4760 administration (Fig. 1E and 1F). Highlighting an anti-inflammatory effect, DIZE decreased also TNF-α, IL-6, and IL-8 mRNA expression and protein content in lung tissues of ALI mice, whereas the opposite effect resulted from MLN-4760 treatment (Fig. 1G-H).

3.2. ACE2 improves EC function in lung tissue from ALI mice

Next, HUVECs were selected as a model to simulate ALI-related EC dysfunction in vitro. To this end, HUVECs were exposed to Poly(I:C) (10 μg/ml, selected after cell viability assays as an optimal, sublethal concentration) for 24 h (Fig. 2A). Consistent with the above in vivo results, after Poly(I:C) stimulation the enzymatic activity and expression of ACE2 protein was decreased, and this change was respectively reversed and enhanced after pre-treatment with DIZE and MLN-4760 (Fig. 2B and 2C). To investigate whether Poly(I:C)-mediated ACE2 downregulation in HUVECs correlated with recruitment of inflammatory cells, the adhesion of calcein-AM-labeled THP-1 monocytes to HUVEC cultures was next examined. After Poly(I:C) stimulation, the number and fluorescence intensity of THP-1 cells that adhered to HUVEC cells was markedly increased. Consistent with a major role of ACE2 in inflammatory cell adhesion to activated ECs, this phenomenon was attenuated and exacerbated, respectively, by pre-treatments with DIZE and MLN-4760 (Fig. 2D and 2E). Using TEER and FITC-dextran clearance assays, we next tested the barrier function of Poly(I:C)-treated HUVECs grown on Transwell inserts. Preliminary experiments examining the relationship between HUVEC growth kinetics and TEER development showed that TEER values remained relatively stable between 48 and 60 h post-seeding (Fig. 2F). During this time window, Poly(I:C) stimulation decreased TEER values, indicating that barrier integrity was damaged. Consistent with protective effects, DIZE increased TEER values and thus improved the EC barrier integrity. Conversely, decreased TEER values, indicative of barrier integrity disruption, were recorded upon MLN-4760 treatment (Fig. 2G). Finally, the permeability coefficient (Pa%) of HUVEC monolayers was estimated through FITC-dextran clearance assays. Results showed that Pa% increased by 85.96 % after Poly(I:C) stimulation, decreased by 43.20 % after DIZE incubation, and increased by 37.10 % after MLN-4760 incubation (Fig. 2H).

3.3. ACE2 alleviates ALI-related EC barrier dysfunction by downregulating FAK/p-FAK expression

Recent research reported that DIZE inhibits lung p-FAK overexpression in a mouse model of pulmonary arterial hypertension (PAH) [41]. Thus, we explored whether DIZE would also modulate FAK/p-FAK protein expression in ECs stimulated with Poly(I:C). FAK/p-FAK protein expression and p-FAK/FAK ratio was elevated in HUVECs following Poly (I:C) stimulation (Fig. 3A). Indicating that ACE2 is involved in the regulation of FAK expression in ECs, DIZE and MLN-4760 downregulated and upregulated, respectively, FAK/p-FAK levels. However, changes in the p-FAK/FAK ratio were not significantly different in Poly (I:C)-treated HUVECs exposed to DIZE and MLN-4760 (Fig. 3B). As expected, treating HUVECs with the FAK inhibitor PF562271 resulted in decreased FAK/p-FAK protein expression and p-FAK/FAK ratio (Fig. 3C). Suggesting a critical role for FAK in ACE2-mediated improvement of ALI-related EC barrier dysfunction, PF562271 enhanced the beneficial effect of DIZE and attenuated the disruptive effect of MLN-4760 by reducing the number and fluorescence intensity of adherent THP-1 cells (Fig. 3D and 3E), increasing TEER values, and decreasing FITC-dextran Pa% by 37.93 % and 47.61 % (Fig. 3F and 3G).

3.4. ACE2 reduces ALI in mice by downregulating FAK/p-FAK expression

We then explored the role of decreased FAK/p-FAK expression in the protective effects of ACE2 on ALI in mice. FAK/p-FAK protein expression was elevated in ALI mice lung tissues, and this effect was counteracted and exacerbated, respectively, after pre-treatment with DIZE and MLN-4760. However, changes in the p-FAK/FAK ratio were not significantly different in Poly(I:C)-treated mice exposed to DIZE and MLN-4760 (Fig. 4A). In addition, and consistent with the in vitro experiments described further above, FAK/p-FAK protein expression and p-FAK/FAK

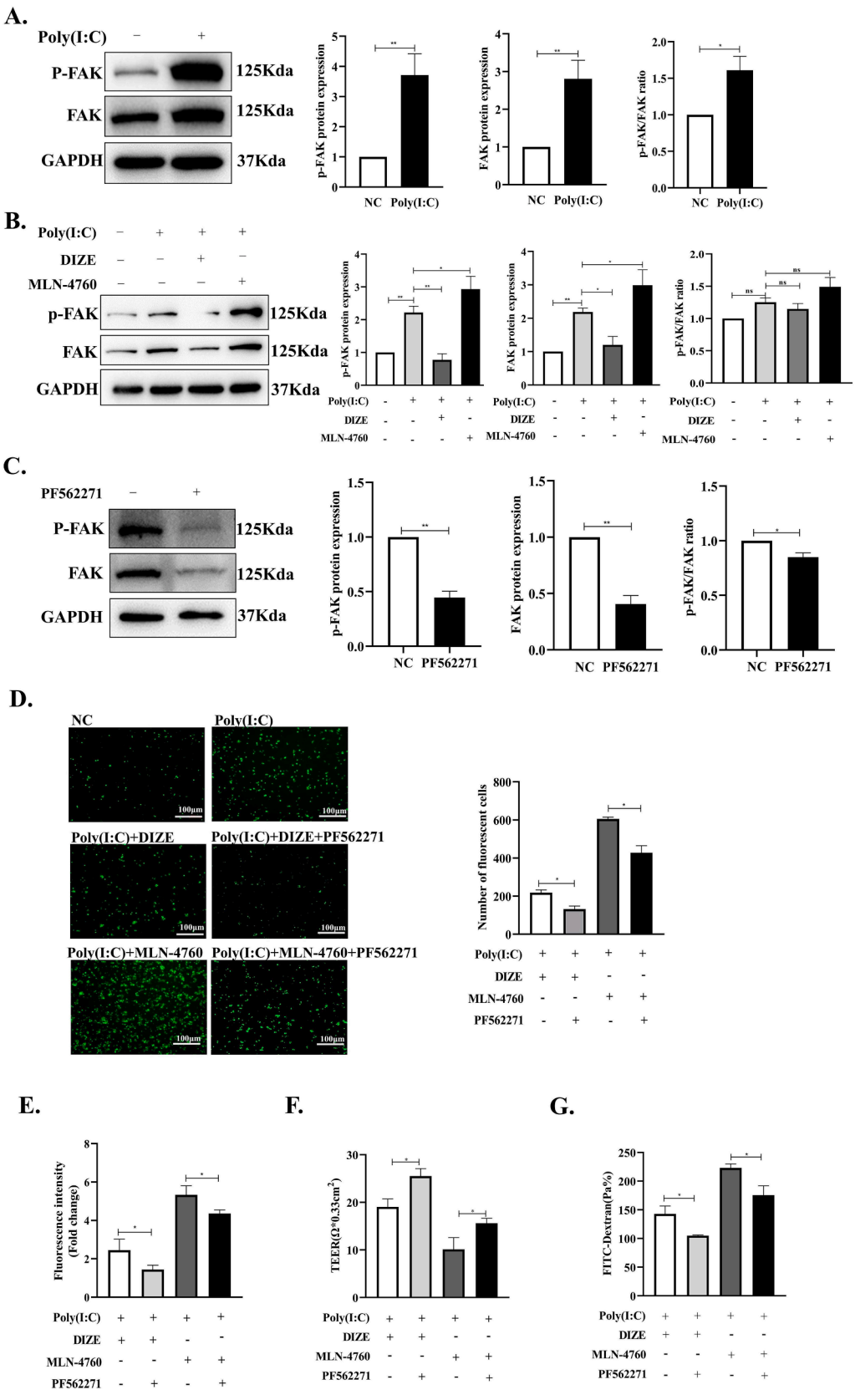

(caption on next page)

Fig. 3. ACE2-mediated FAK/p-FAK downregulation reduces monocyte adhesion and improves barrier function in Poly (I:C)-treated HUVECs. (A) Western blot analysis of FAK/p-FAK expression and p-FAK/FAK ratio in NC and Poly(I:C)-treated HUVECs. (B) Western blot analysis of FAK/p-FAK expression and p-FAK/FAK ratio in Poly(I:C)-treated HUVECs exposed to DIZE and MLN-4760. (C) Western blot analysis of FAK/p-FAK expression and p-FAK/FAK ratio in NC or PF562271-treated HUVECs. (D) Effect of PF562271 on the number of THP-1 cells adhering to Poly(I:C)-treated HUVECs exposed to DIZE and MLN-4760. (E) Effect of PF562271 on the calcein-AM fluorescence intensity of THP-1 cells adhering to Poly(I:C)-treated HUVECs exposed to DIZE and MLN-4760. (F) Effect of PF562271 on TEER values in Poly(I:C)-treated HUVECs. (G) Alterations in permeability coefficients (Pa%) of FITC-dextran in HUVECs treated with PF562271. $^{*}P < 0.05$; $^{**}P < 0.01$; $^{***}P < 0.001$. N = 3 independent experiments.

ratio was significantly reduced in mouse lung tissues upon treatment with PF562271 (Fig. 4B). As expected, PF562271 enhanced the protective effect of DIZE against ALI by further reducing alveolar wall thickness alveolar vacuolization, inflammatory and erythrocyte infiltration of alveolar interstitium, and interstitial edema and congestion, and the lung injury score strongly supports this conclusion (Fig. 4C), and reduced the lung wet/dry weight ratio, BALF's total protein content, and TNF-α, IL-6, and IL-8 mRNA expression and protein content (Fig. 4D-G).

3.5. ACE2 decreases endothelial FAK/p-FAK expression by stimulating the ANG1-7/MAS axis

We next explored the molecular mechanism by which ACE2 downregulates FAK/p-FAK protein expression. ACE2 hydrolyzes ANGII to generate ANG1-7, which binds to downstream MAS receptors to exert vasculoprotective effects [16]. It was reported that ANG II promotes FAK expression and activation in intestinal and cardiovascular disease models [38–40]. Therefore, we tested whether ACE2 downregulates FAK/p-FAK expression through the ANG1-7-MAS axis. Western blot analyses in HUVECs indicated that Poly(I:C) treatment downregulated ANG1-7 and MAS protein expression, and this expression trend was reversed and enhanced, respectively, by DIZE and MLN-4760 (Fig. 5A and 5B). To verify the role of the ANG1-7-MAS axis in the downregulation of FAK/p-FAK expression mediated by ACE2, HUVECs were transfected with small interfering RNA (siRNA) targeting MAS (si-MAS) and subsequently treated with ANG1-7. Western blot results showed that ANG1-7 inhibited FAK/p-FAK protein expression compared with the DIZE-treated and MLN-4760-treated groups. However, there was no significant difference in the change of p-FAK/FAK ratio (Fig. 5C). In turn, MAS protein downregulation (Fig. 5D), paralleled by upregulated FAK/p-FAK protein expression (Fig. 5E), were detected via western blotting in si-MAS-transfected, compared to si-NC-transfected, HUVECs. However, changes in the p-FAK/FAK ratio were not significantly different in HUVECs transfected with si-NC and si-MAS.

3.6. ACE2 activates the ANG 1–7/MAS axis and downregulates FAK/p-FAK expression in lung tissue from ALI mice

Finally, we explored whether ACE2 downregulates FAK/p-FAK protein expression in vivo through the ANG1-7-MAS axis. Consistent with the above HUVEC experiments, in Poly(I:C) treated lung tissues ANG1-7 and MAS protein expression was reduced, and this effect was reversed by DIZE and magnified by MLN-4760 (Fig. 6A and 6B). We further studied FAK/p-FAK expression after treating mice with ANG1-7 and the MAS receptor inhibitor A779. Western blot results showed that compared with the DIZE-treated group, ANG1-7 downregulated, while A779 upregulated, FAK/p-FAK protein expression in the lungs of Poly(I:C)-treated mice. On the other hand, compared with the MLN-4760-treated group, FAK/p-FAK protein expression was downregulated by ANG1-7 and upregulated by A779. However, there was no significant difference between the effects of ANG1-7 and A779 on the change of p-FAK/FAK ratio (Fig. 6C and 6D). These findings therefore indicate that pharmacological activation of ACE2 decreases FAK/p-FAK expression levels via Ang1-7-Mas axis regulation, leading to improved EC function and reduced lung damage in ALI mice. A schematic depiction of the molecular mechanisms intervening in ACE2-mediated ALI attenuation is shown in Fig. 7.

4. Discussion

Increased expression of adhesion molecules in ECs and impaired EC barrier function are critical determinants of ALI. The number of leukocytes adhering to ECs is increased during ALI, which allows leukocyte migration across the capillary lung endothelium. Concomitantly, an impaired EC barrier function increases vascular permeability and leads to alveolar collapse [32,42,43]. SARS-COV-2 infection induces also platelet activation, triggering a coagulation cascade that accelerates thrombosis. In this way, and aided by increased vascular permeability, a vasculopathy develops which ultimately accelerates the development of ALI [44,45]. Therefore, restoration of EC function represents an enticing target for ALI treatment.

Poly(I:C), a synthetic analogue of double-stranded RNA, is often utilized to mimic viral infections, as it leads to activation of immune responses in cells and tissues [46]. While a normal, mild immune response typically has an antiviral effect, an excessive immune response can lead to inflammation [8,9]. Poly(I:C) was shown to induce virus-like inflammation in neural, liver, and lung/airway tissues [10–13]. Our previous study showed that Poly(I:C) effectively induces ALI in mice, and increases the permeability of lung ECs [14]. In our current study, we observed an increase in the number and fluorescence intensity of THP-1 monocytes adhering to Poly(I:C)-stimulated HUVECs. This was paralleled by decreased TEER and increased FITC-dextran clearance in HUVEC monolayers, indicating that Poly(I:C) leads to inflammatory immune cell adhesion and increases the permeability of ECs.

Endothelial ACE2 is critically involved in COVID-19-related ALI [45], as the binding of the RBD sequence of the S protein on the surface of SARS-COV-2 to ACE2 mediates the entry of the virus into the respiratory tract [47,48]. ACE2 acts as a central regulator of the two major axes of the RAS system, as it hydrolyzes ANG II, which exerts pro-inflammatory effects by binding to ATR1, into ANG1-7, which binds to MAS receptors to exert anti-inflammatory actions [49]. Dysregulation of ACE2 leads to the disruption of the RAS system and the local microenvironment, and eventually causes the development of inflammation [16]. Some studies have shown that abnormal ACE2 expression occurs in human cells during SARS-COV-2 infection. In airway epithelial cells, SARS-COV-2 induces interferon (IFN) expression, which in turn promotes ACE2 overexpression. Elevated expression of ACE2 further accelerates the invasion of SARS-COV-2 in a positive-feedback manner [19]. However, studies have shown that after SARS-COV-2 infection, ACE2 expression in alveolar ECs is lower than in healthy individuals [50]. In this regard, evidence shows that ACE2-mediated SARS-COV-2 infection activates ADAM-17, which leads to decreased ACE2 expression and ultimately causes dysregulation of the RAS system, resulting in severe lung disease [51,52]. Experiments in rodents indicated also that SARS-COV-2 infection can directly lead to decreased ACE2 expression in lung tissues, and the use of drugs that increase ACE2 enzyme activity alleviates lung injury [53]. Given that dysregulation of ACE2 expression entails deleterious effects on tissues and cells, we hypothesized that severe EC dysfunction in ALI may be related to dysregulation of ACE2 expression. Our results showed that ACE2 expression and ACE2 enzyme activity was decreased in both in vivo and cell-based models of ALI induced by Poly(I:C). This is consistent with changes in ACE2 expression occurring in ALI models induced by other agents and factors such as LPS, acid inhalation and sepsis [54–56]. In addition, ACE2 protein expression is decreased upon development of lung fibrosis and kidney injury [57,58]. The demonstration that the phenomenon of decreased ACE2 is

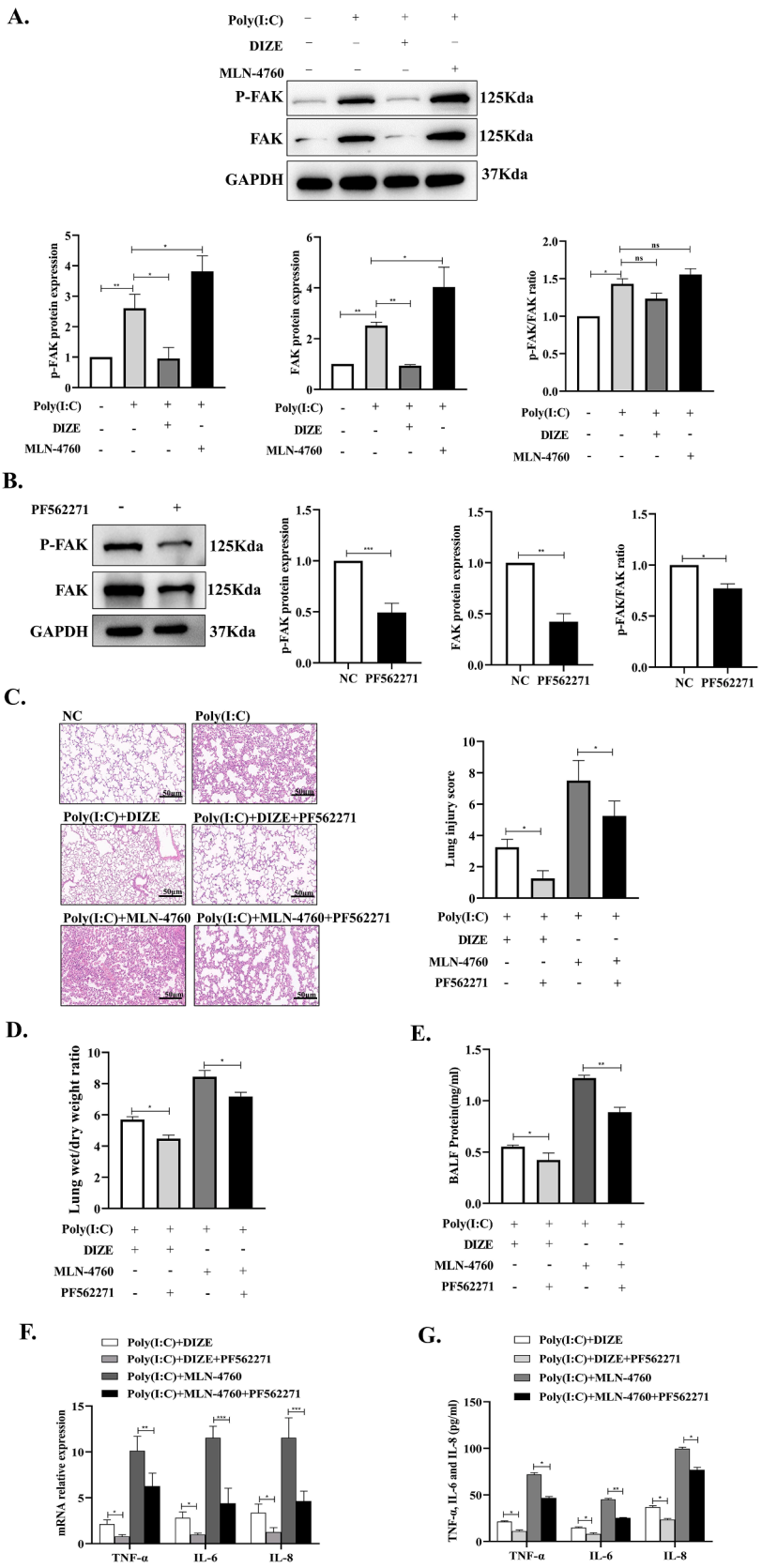

Fig. 4. ACE2 expression attenuates ALI by downregulating FAK/p-FAK expression. (A) Western blot analysis of FAK/p-FAK expression and p-FAK/FAK ratio in lung tissues from DIZE- and and MLN-4760-treated ALI mice. (B) Western blot analysis of FAK/p-FAK expression and p-FAK/FAK ratio in NC or PF562271-treated mice. (C) Effect of PF562271 on lung histopathology and lung injury scores in DIZE- and MLN-4760- treated ALI mice. (D, E) Lung wet/dry weight ratio and BALF total protein concentration in PF562271-treated ALI mice exposed to DIZE and MLN-4760. (F) Analysis of TNF-α, IL-6, and IL-8 mRNA expression changes in lung tissues from PF562271-treated ALI mice exposed to DIZE and MLN-4760. (G) ELISA was used to detect the levels of TNF-α, IL-6, and IL-8 expression in lung tissues from PF562271-treated ALI mice exposed to DIZE and MLN-4760. $^{*}P < 0.05$; $^{**}P < 0.01$; $^{***}P < 0.001$. N = 4 mice per group.

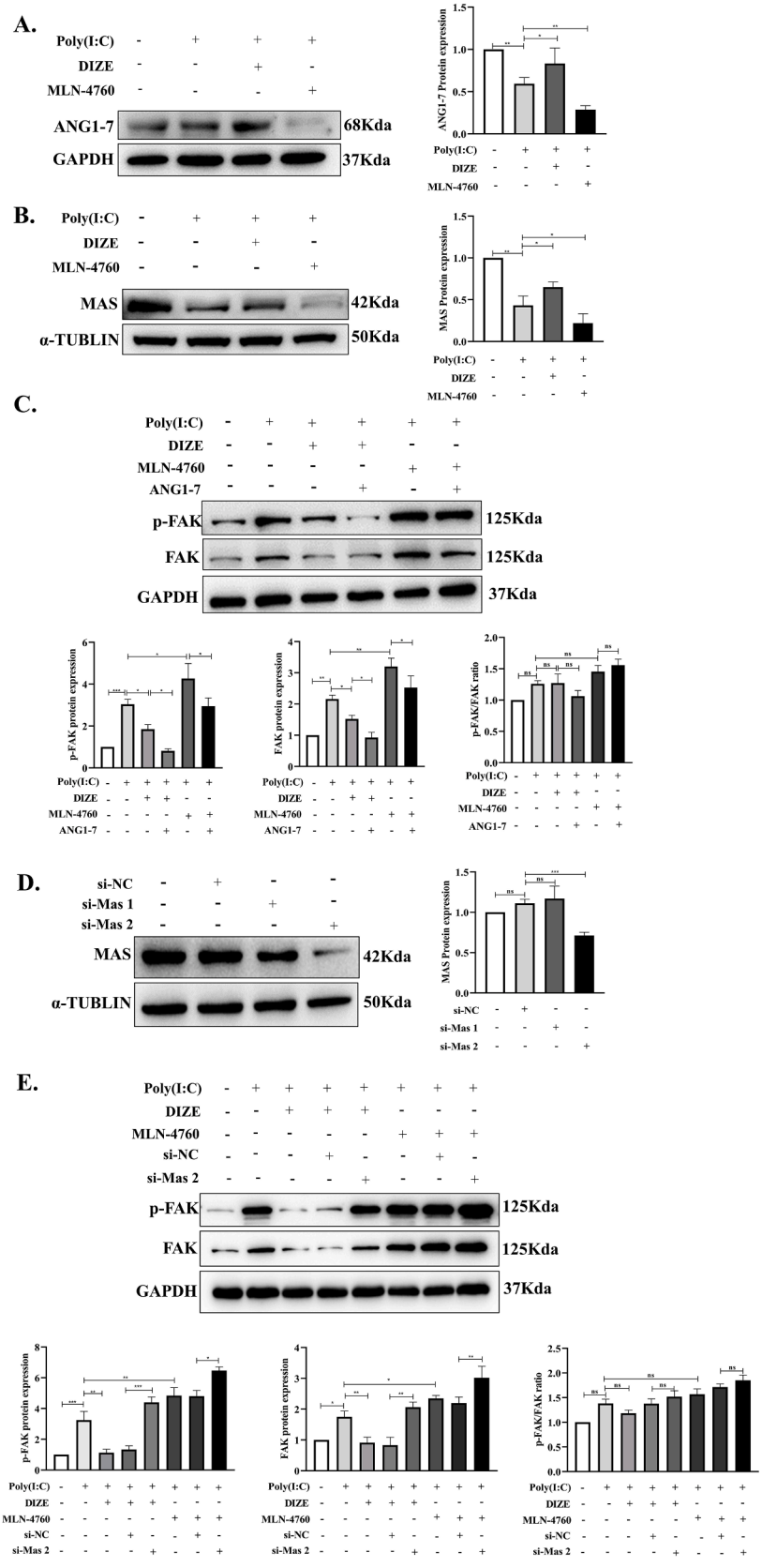

Fig. 5. ACE2-mediated stimulation of the ANG 1–7/MAS axis decreases endothelial FAK/p-FAK expression. (A, B) Western blot analysis of ANG 1–7 and MAS expression in Poly(I:C)-treated HUVECs exposed to DIZE and MLN-4760. (C) Western blot analysis of the effect of ANG1-7 on FAK/p-FAK expression and p-FAK/FAK ratio levels in Poly(I:C)-treated HUVECs exposed to DIZE and MLN-4760. (D) Western blot analysis of MAS protein knockdown efficiency upon transient transfection of MAS-targeted siRNA (siMAS) into HUVECs. (E) Western blot analysis of FAK/p-FAK expression and p-FAK/FAK ratio in HUVECs transfected with si-NC and si-MAS. $*P < 0.05$; $**P < 0.01$; $***P < 0.001$. N = 3 independent experiments.

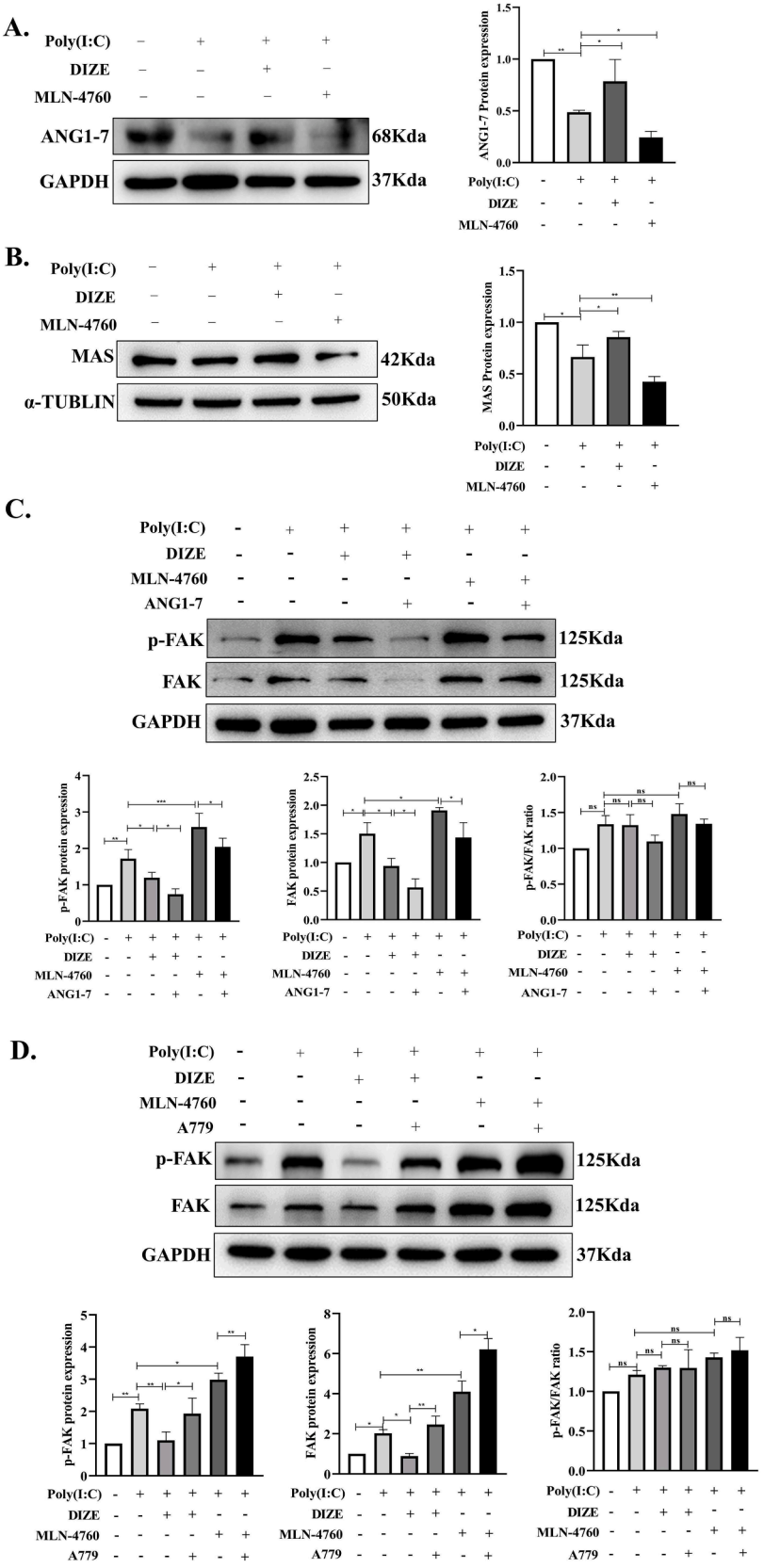

Fig. 6. ACE2-mediated stimulation of the ANG 1–7/MAS axis downregulates FAK/p-FAK expression in mouse lung tissue. (A, B) Western blot analysis of ANG 1–7 and MAS expression in lung tissues form ALI mice treated with DIZE and MLN-4760. (C) Western blot analysis of FAK/p-FAK expression and p-FAK/FAK ratio in lung tissues from ALI mice treated with ANG1-7 and DIZE or MLN-4760. (D) Western blot analysis of FAK/p-FAK expression and p-FAK/FAK ratio in lung tissues of ALI mice treated with the MAS receptor inhibitor A779 and DIZE or MLN-4760. $*P < 0.05$; $**P < 0.01$; $***P < 0.001$. N = 4 mice per group.

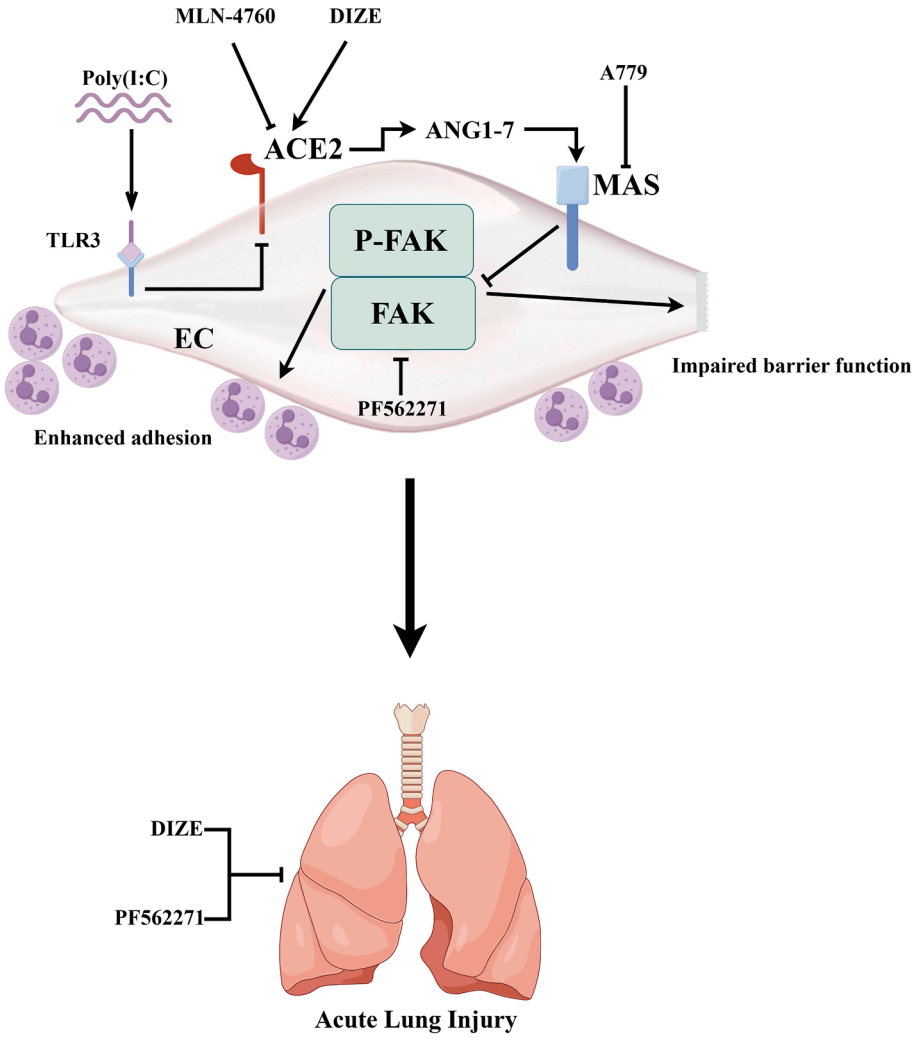

Fig. 7. Summary schematic of the proposed mechanism by which the ACE2 agonist DIZE improves EC function and alleviates ALI in mice. Drawing by Figdraw (www.figdraw.com).

not only seen after SARS-COV-2 infection, but also in several other inflammatory diseases, suggests the importance of ACE2 downregulation in the development of inflammatory conditions.

DIZE, a small-molecule antiprotozoal drug with ACE2 activating properties [59], was shown to have beneficial effects in experimental models of hypertension, myocardial infarction, type 1 diabetes mellitus, and atherosclerosis [23,60,61]. Whereas the therapeutic effects of DIZE had not been so far tested in animal models of Poly(I:C)-induced ALI, DIZE was reported to reduce pulmonary fibrosis to alleviate ischemia–reperfusion-induced ALI [62,63]. We also used MLN-4760, a highly specific ACE2 inhibitor [64], to downregulate ACE2 expression in vivo and in vitro. We confirmed that upregulation of ACE2 expression and enhancement of ACE2 enzyme activity by DIZE alleviated Poly(I:C)-induced ALI, as evidenced by decreased lung tissue damage, diminished EC adhesion capacity, and restoration of endothelial barrier function. In contrast, downregulation of ACE2 expression by MLN-4760 exacerbated Poly(I:C)-induced ALI, as evidenced by increased lung tissue damage, enhanced EC adhesion capacity, and further disruption of endothelial barrier function. Therefore, the upregulation of ACE2 by DIZE may serve as a therapeutic strategy for ALI.

Considering that ACE2 expression in epithelial/endothelial is crucial for viral respiratory infection and subsequent development of ALI, our investigation of the molecular mechanisms by which upregulated ACE2 expression alleviates ALI focused on potential changes in EC adhesive properties and barrier function. The features of focal adhesions (FAs), complex macromolecular structures that tightly connect the cytoskeleton of cells to the extracellular matrix, are well established [65]. FAs regulate important EC activities, including adhesion, migration, proliferation, and barrier function [66]. The composition of FAs, as well as the signaling pathways mediated by these complexes, are dependent on the activation of FAK [67]. In pathological conditions, FAK overactivation triggers cellular dysfunction by altering fundamental cell processes. For instance, FAK is highly expressed in several tumors, and promotes the proliferation and migration of melanoma and gastric cancer cells [30,31]. Inhibition of FAK activation reduces the expression of the cell surface adhesion molecules ICAM-1 and VCAM-1, which inhibits in turn inflammatory cell adhesion to ECs [68]. Furthermore, inhibition of FAK activation promotes the restoration of the endothelial barrier function and decreases ROS expression and mitochondrial damage in an ischemia–reperfusion-treated Bend.3 cell model [69]. In this study, we showed that ACE2 activation improves EC function and alleviates Poly(I:C)-induced ALI in mice by reducing FAK/p-FAK protein expression. Our experiments using ANG 1–7 hinted that this effect is related to mechanisms involved in RAS signaling, in line with evidence that ANGII promotes FAK activation during the development of cardiomyopathy and cardiovascular disease [38–40]. It is thus apparent that FAK activation by ANG II contributes to ALI development, which would be restricted by conversion of ANGII into ANG 1–7 by ACE2 to inhibit FAK activation. Our results are indeed consistent with those obtained in a rat pulmonary arterial hypertension (PAH) model, where DIZE inhibited p-FAK protein

expression [41]. We also showed that ANG 1–7/MAS protein expression was decreased, along with that of ACE2, in both lung tissue from ALI mice and in Poly(I:C)-treated HUVECs in culture. In a rat model of Alzheimer's disease, DIZE treatment promoted ANG1-7 expression and activated the MAS receptor, resulting in increase of acetylcholine levels [70]. Our study showed that the ACE2 activator DIZE upregulated ANG1-7 and MAS expression and decreased FAK/p-FAK expression both in lungs from ALI and mice and in Poly(I:C)-treated ECs, indicating a correlation between ANG 1–7/MAS axis activation and ACE2-induced FAK/p-FAK downregulation in ALI.

Our studies strongly suggest that FAK is a potential target for the treatment of ALI. Several small-molecule FAK inhibitors have shown to specifically suppress FAK expression or activation, and are currently being used to inhibit the migration and proliferation of tumor cells [71]. Another FAK inhibitor, PF562271, was evaluated for safety in 99 patients with solid tumors (mainly head and neck, prostate and pancreatic cancers) in a phase I clinical trial that demonstrated that the compound was generally well tolerated [36]. Interestingly, the FAK inhibitor PND-1186 was shown to inhibit the macrophage-mediated inflammatory response and thus alleviate LPS-induced ALI in mice [72]. In our Poly(I:C)-induced mouse model of ALI associated with impaired EC function, the therapeutic effect of DIZE was effectively enhanced upon administration of PF562271.

In summary, we showed that ACE2 activity downregulates FAK/p-FAK protein expression through the ANG 1–7/MAS axis in both mouse lung tissues and cultured ECs. Specifically, we demonstrated that the ACE2 activator DIZE, as well as the FAK inhibitor PF562271, alleviate Poly(I:C)-induced ALI in mice and improves EC barrier function and reduces the adhesion of immune inflammatory cells to ECs. This study presents some limitations. It is well known that FAK is expressed and regulates numerous pathophysiological processes in multiple cell types, including ECs and inflammatory immune cells [73,74]. Thus, additional experiments are warranted to determine the specific targets and mechanisms through which FAK inhibition attenuates ALI severity. We propose that DIZE in combination with PF562271 may represent a new therapeutic strategy for the treatment of ALI and ARDS. In future research, we plan to validate the results of this study using mouse lung ECs.

Funding

This project was supported financially by the National Natural Science Foundation of China (NSFC) Grants 82104178 and the Natural Science Research Project of Anhui Educational Committee, Grants KJ2021A0768 (W. Gu). Bengbu Medical College Scientific and Technology Self-Innovation Foundation Program, Grants BYKC201903 (G. Liu). Innovation Training Program for College Students in Anhui Province, Grants S202210367012 (J. Pan).

CRediT authorship contribution statement

Yixuan He: Writing – original draft, Writing – review & editing, Data curation. **Baocai Gang:** Data curation, Software. **Mengjie Zhang:** Data curation, Visualization. **Yuting Bai:** Data curation, Visualization. **Ziyu Wan:** Data curation, Visualization. **Jiesong Pan:** Data curation. **Jie Liu:** Supervision. **Guoquan Liu:** Conceptualization, Methodology, Writing – review & editing. **Wei Gu:** Conceptualization, Methodology, Writing – original draft, Writing – review & editing.

Declaration of competing interest

The authors declare that they have no known competing financial interests or personal relationships that could have appeared to influence the work reported in this paper.

Data availability

Data will be made available on request.

Acknowledgment

Not applicable.

Appendix A. Supplementary material

Supplementary data to this article can be found online at https://doi.org/10.1016/j.intimp.2024.111535.

References

[1] D. Mokra, Acute lung injury - from pathophysiology to treatment, Physiol. Res. 69 (Suppl 3) (2020) S353–S366.
[2] L. Wang, Y. Cao, B. Gorshkov, Y. Zhou, Q. Yang, J. Xu, Q. Ma, X. Zhang, J. Wang, X. Mao, X. Zeng, Y. Su, A.D. Verin, M. Hong, Z. Liu, Y. Huo, Ablation of endothelial Pfkfb3 protects mice from acute lung injury in LPS-induced endotoxemia, Pharmacol. Res. 146 (2019) 104292.
[3] E.E. Friedrich, Z. Hong, S. Xiong, M. Zhong, A. Di, J. Rehman, Y.A. Komarova, A. B. Malik, Endothelial cell Piezo1 mediates pressure-induced lung vascular hyperpermeability via disruption of adherens junctions, Proc. Natl. Acad. Sci. USA 116 (26) (2019) 12980–12985.
[4] E.J. Debruin, M.R. Hughes, C. Sina, A. Lu, J. Cait, Z. Jian, M. Lopez, B. Lo, T. Abraham, K.M. McNagny, Podocalyxin regulates murine lung vascular permeability by altering endothelial cell adhesion, PLoS One 9 (10) (2014) e108881.
[5] L. Li, J. Wei, R.K. Mallampalli, Y. Zhao, J. Zhao, TRIM21 Mitigates Human Lung Microvascular Endothelial Cells' Inflammatory Responses to LPS, Am. J. Respir. Cell Mol. Biol. 61 (6) (2019) 776–785.
[6] J.P. Robles, M. Zamora, E. Adan-Castro, L. Siqueiros-Marquez, G. Martinez de la Escalera, C. Clapp, The spike protein of SARS-CoV-2 induces endothelial inflammation through integrin alpha5beta1 and NF-kappaB signaling, J. Biol. Chem. 298 (3) (2022) 101695.
[7] A. Birnhuber, E. Fliesser, G. Gorkiewicz, M. Zacharias, B. Seeliger, S. David, T. Welte, J. Schmidt, H. Olschewski, M. Wygrecka, G. Kwapiszewska, Between inflammation and thrombosis: endothelial cells in COVID-19, Eur. Respir. J. 58 (3) (2021).
[8] N.E. Martins, Towards a Mechanism for Poly(I.C) Antiviral Priming in Oysters, MBio 11 (2) (2020).
[9] N.C. Stowell, J. Seideman, H.A. Raymond, K.A. Smalley, R.J. Lamb, D.D. Egenolf, P.J. Bugelski, L.A. Murray, P.A. Marsters, R.A. Bunting, R.A. Flavell, L. Alexopoulou, L.R. San Mateo, D.E. Griswold, R.T. Sarisky, M.L. Mbow, A.M. Das, Long-term activation of TLR3 by poly(I:C) induces inflammation and impairs lung function in mice, Respir. Res. 10 (1) (2009) 43.
[10] Z. Xie, H. Zhou, M. Obana, Y. Fujio, N. Okada, M. Tachibana, Myeloid-derived suppressor cells exacerbate poly(I:C)-induced lung inflammation in mice with renal injury and older mice, Front. Immunol. 14 (2023) 1243851.
[11] X.M. Li, T.Y. Yang, X.S. He, J.R. Wang, W.J. Gan, S. Zhang, J.M. Li, H. Wu, Orphan nuclear receptor Nur77 inhibits poly (I:C)-triggered acute liver inflammation by inducing the ubiquitin-editing enzyme A20, Oncotarget 8 (37) (2017) 61025–61035.
[12] S. Arora, S. Gupta, W. Akram, A.E. Altyar, P. Tagde, Effect of TLR3/dsRNA complex inhibitor on Poly(I:C)-induced airway inflammation in Swiss albino mice, Environ. Sci. Pollut. Res. Int. 30 (10) (2023) 28118–28132.
[13] R. Field, S. Campion, C. Warren, C. Murray, C. Cunningham, Systemic challenge with the TLR3 agonist poly I: C induces amplified IFNalpha/beta and IL-1beta responses in the diseased brain and exacerbates chronic neurodegeneration, Brain Behav. Immun. 24 (6) (2010) 996–1007.
[14] L. Zhang, Y. Ye, H. Kang, J. Pan, Q. Xu, H. Zhu, G. Liu, W. Gu, Comparative studies of mouse acute lung injury models induced by lipopolysaccharide and polyinosinic-polycytidylic acid, J. Biol. Regul. Homeost. Agents 36 (2) (2022) 353–362.
[15] P. Herrera, R.J. Cauchi, ACE and ACE2: insights from Drosophila and implications for COVID-19, Heliyon 7 (12) (2021) e08555.
[16] E. Cantero-Navarro, B. Fernandez-Fernandez, A.M. Ramos, S. Rayego-Mateos, R. R. Rodrigues-Diez, M.D. Sanchez-Nino, A.B. Sanz, M. Ruiz-Ortega, A. Ortiz, Renin-angiotensin system and inflammation update, Mol. Cell. Endocrinol. 529 (2021) 111254.
[17] K.Y. Shim, Y.W. Eom, M.Y. Kim, S.H. Kang, S.K. Baik, Role of the renin-angiotensin system in hepatic fibrosis and portal hypertension, Korean J. Intern. Med. 33 (3) (2018) 453–461.
[18] Q.Q. Zhang, F.H. Chen, F. Wang, X.M. Di, W. Li, H. Zhang, A Novel Modulator of the Renin-Angiotensin System, Benzoylaconitine, Attenuates Hypertension by Targeting ACE/ACE2 in Enhancing Vasodilation and Alleviating Vascular Inflammation, Front. Pharmacol. 13 (2022) 841435.
[19] C.G. Ziegler, S.J. Allon, S.K. Nyquist, I.M. Mbano, V.N. Miao, C.N. Tzouanas, Y. Cao, A.S. Yousif, J. Bals, B.M. Hauser, J. Feldman, SARS-CoV-2 Receptor ACE2 Is an Interferon-Stimulated Gene in Human Airway Epithelial Cells and Is Detected in Specific Cell Subsets across Tissues, Cell 181 (5) (2020) 1016–1035.e19.

[20] M. Gheblawi, K. Wang, A. Viveiros, Q. Nguyen, J.C. Zhong, A.J. Turner, M. K. Raizada, M.B. Grant, G.Y. Oudit, Angiotensin-Converting Enzyme 2: SARS-CoV-2 Receptor and Regulator of the Renin-Angiotensin System: Celebrating the 20th Anniversary of the Discovery of ACE2, Circ. Res. 126 (10) (2020) 1456–1474.
[21] A. Kumar, R.K. Narayan, C. Kumari, M.A. Faiq, M. Kulandhasamy, K. Kant, V. Pareek, SARS-CoV-2 cell entry receptor ACE2 mediated endothelial dysfunction leads to vascular thrombosis in COVID-19 patients, Med. Hypotheses 145 (2020) 110320.
[22] K. Wang, M. Gheblawi, A. Nikhanj, M. Munan, E. MacIntyre, C. O'Neil, M. Poglitsch, D. Colombo, F. Del Nonno, Z. Kassiri, W. Sligl, G.Y. Oudit, Dysregulation of ACE (Angiotensin-Converting Enzyme)-2 and Renin-Angiotensin Peptides in SARS-CoV-2 Mediated Mortality and End-Organ Injuries, Hypertension 79 (2) (2022) 365–378.
[23] V. Shenoy, A. Gjymishka, Y.P. Jarajapu, Y. Qi, A. Afzal, K. Rigatto, A.J. Ferreira, R. A. Fraga-Silva, P. Kearns, J.Y. Douglas, D. Agarwal, K.K. Mubarak, C. Bradford, W. R. Kennedy, J.Y. Jun, A. Rathinasabapathy, E. Bruce, D. Gupta, A.J. Cardounel, J. Mocco, J.M. Patel, J. Francis, M.B. Grant, M.J. Katovich, M.K. Raizada, Diminazene attenuates pulmonary hypertension and improves angiogenic progenitor cell functions in experimental models, Am. J. Respir. Crit. Care Med. 187 (6) (2013) 648–657.
[24] C. Castardeli, C.L. Sartorio, E.B. Pimentel, L. Forechi, J.G. Mill, The ACE 2 activator diminazene aceturate (DIZE) improves left ventricular diastolic dysfunction following myocardial infarction in rats, Biomed. Pharmacother. 107 (2018) 212–218.
[25] T. Qaradakhi, L. Gadanec, J. Matsoukas, V. Apostolopoulos, A. Zulli, Could DIZE be the answer to COVID-19? Maturitas 140 (2020) 83–84.
[26] Y.G. Mishra, B. Manavathi, Focal adhesion dynamics in cellular function and disease, Cell. Signal. 85 (2021) 110046.
[27] J. Le Coq, I. Acebron, B. Rodrigo Martin, P. Lopez Navajas, D. Lietha, New insights into FAK structure and function in focal adhesions, J. Cell Sci. 135 (20) (2022).
[28] P. Tapial Martinez, P. Lopez Navajas, D. Lietha, FAK Structure and Regulation by Membrane Interactions and Force in Focal Adhesions, Biomolecules 10 (2) (2020).
[29] W. Gu, L. Zhang, X. Zhang, B. Wang, X. Shi, K. Hu, Y. Ye, G. Liu, MiR-15p-5p Mediates the Coordination of ICAM-1 and FAK to Promote Endothelial Cell Proliferation and Migration, Inflammation 45 (3) (2022) 1402–1417.
[30] A. Mousson, M. Legrand, T. Steffan, R. Vauchelles, P. Carl, J.P. Gies, M. Lehmann, G. Zuber, J. De Mey, D. Dujardin, E. Sick, P. Ronde, Inhibiting FAK-Paxillin Interaction Reduces Migration and Invadopodia-Mediated Matrix Degradation in Metastatic Melanoma Cells, Cancers (basel) 13 (8) (2021).
[31] Y. Ma, Y. Fu, X. Fan, Q. Ji, X. Duan, Y. Wang, Y. Zhang, Z. Wang, H. Hao, FAK/IL-8 axis promotes the proliferation and migration of gastric cancer cells, Gastric Cancer 26 (4) (2023) 528–541.
[32] S.A. Parsons, R. Sharma, D.L. Roccamatisi, H. Zhang, B. Petri, P. Kubes, P. Colarusso, K.D. Patel, Endothelial paxillin and focal adhesion kinase (FAK) play a critical role in neutrophil transmigration, Eur J Immunol 42 (2) (2012) 436–446.
[33] S. Yang, R. Yip, S. Polena, M. Sharma, S. Rao, P. Griciene, J. Gintautas, H. Jerome, Reactive oxygen species increased focal adhesion kinase production in pulmonary microvascular endothelial cells, Proc. West. Pharmacol. Soc. 47 (2004) 54–56.
[34] E. Kurenova, D. Ucar, J. Liao, M. Yemma, P. Gogate, W. Bshara, U. Sunar, M. Seshadri, S.N. Hochwald, W.G. Cance, A FAK scaffold inhibitor disrupts FAK and VEGFR-3 signaling and blocks melanoma growth by targeting both tumor and endothelial cells, Cell Cycle 13 (16) (2014) 2542–2553.
[35] L. Zhang, D. Zhao, Y. Wang, W. Zhang, J. Zhang, J. Fan, Q. Zhan, J. Chen, Focal adhesion kinase (FAK) inhibitor-defactinib suppresses the malignant progression of human esophageal squamous cell carcinoma (ESCC) cells via effective blockade of PI3K/AKT axis and downstream molecular network, Mol. Carcinog. 60 (2) (2021) 113–124.
[36] A. Schultze, W. Fiedler, Clinical importance and potential use of small molecule inhibitors of focal adhesion kinase, Anticancer Agents Med. Chem. 11 (7) (2011) 593–599.
[37] N.E. Clarke, M.J. Fisher, K.E. Porter, D.W. Lambert, A.J. Turner, Angiotensin converting enzyme (ACE) and ACE2 bind integrins and ACE2 regulates integrin signalling, PLoS One 7 (4) (2012) e34747.
[38] H. Zheng, X. Li, X. Zeng, C. Huang, M. Ma, X. Lv, Y. Zhang, L. Sun, G. Wang, Y. Du, Y. Guan, TMEM16A inhibits angiotensin II-induced basilar artery smooth muscle cell migration in a WNK1-dependent manner, Acta Pharm. Sin. B 11 (12) (2021) 3994–4007.
[39] H. Nakashima, H. Suzuki, H. Ohtsu, J.Y. Chao, H. Utsunomiya, G.D. Frank, S. Eguchi, Angiotensin II regulates vascular and endothelial dysfunction: recent topics of Angiotensin II type-1 receptor signaling in the vasculature, Curr. Vasc. Pharmacol. 4 (1) (2006) 67–78.
[40] X. Jiang, J. Sinnett-Smith, E. Rozengurt, Differential FAK phosphorylation at Ser-910, Ser-843 and Tyr-397 induced by angiotensin II, LPA and EGF in Intestinal Epithelial Cells, Cell Signal 19 (5) (2007) 1000–1010.
[41] R. Wang, J. Xu, J. Wu, S. Gao, Z. Wang, Angiotensin-converting enzyme 2 alleviates pulmonary artery hypertension through inhibition of focal adhesion kinase expression, Exp. Ther. Med. 22 (4) (2021) 1165.
[42] S. Nourshargh, R. Alon, Leukocyte migration into inflamed tissues, Immunity 41 (5) (2014) 694–707.
[43] R. Lucas, A.D. Verin, S.M. Black, J.D. Catravas, Regulators of endothelial and epithelial barrier integrity and function in acute lung injury, Biochem. Pharmacol. 77 (12) (2009) 1763–1772.
[44] L.C. Barbosa, T.L. Goncalves, L.P. de Araujo, L.V.O. Rosario, V.P. Ferrer, Endothelial cells and SARS-CoV-2: An intimate relationship, Vasc.Pharmacol. 137 (2021) 106829.
[45] R.M.L. Colunga Biancatelli, P.A. Solopov, E.R. Sharlow, J.S. Lazo, P.E. Marik, J. D. Catravas, The SARS-CoV-2 spike protein subunit S1 induces COVID-19-like acute lung injury in Kappa18-hACE2 transgenic mice and barrier dysfunction in human endothelial cells, Am. J. Physiol. Lung Cell. Mol. Physiol. 321 (2) (2021) L477–L484.
[46] C. Guo, J.Z. Ye, M. Song, X.X. Peng, H. Li, Poly I: C promotes malate to enhance innate immune response against bacterial infection, Fish Shellfish Immunol. 131 (2022) 172–180.
[47] C.T. Baldari, A. Onnis, E. Andreano, G. Del Giudice, R. Rappuoli, Emerging roles of SARS-CoV-2 Spike-ACE2 in immune evasion and pathogenesis, Trends Immunol. 44 (6) (2023) 424–434.
[48] U.M. Ashraf, A.A. Abokor, J.M. Edwards, E.W. Waigi, R.S. Royfman, S.A. Hasan, K. B. Smedlund, A.M.G. Hardy, R. Chakravarti, L.G. Koch, SARS-CoV-2, ACE2 expression, and systemic organ invasion, Physiol. Genomics 53 (2) (2021) 51–60.
[49] A. Kaparianos, E. Argyropoulou, Local renin-angiotensin II systems, angiotensin-converting enzyme and its homologue ACE2: their potential role in the pathogenesis of chronic obstructive pulmonary diseases, pulmonary hypertension and acute respiratory distress syndrome, Curr. Med. Chem. 18 (23) (2011) 3506–3515.
[50] S. Panigrahi, T. Goswami, B. Ferrari, C.J. Antonelli, D.A. Bazdar, H. Gilmore, M. L. Freeman, M.M. Lederman, S.F. Sieg, SARS-CoV-2 Spike Protein Destabilizes Microvascular Homeostasis, Microbiol. Spectr. 9 (3) (2021) e0073521.
[51] Y. Miura, H. Ohkubo, A. Nakano, J.E. Bourke, S. Kanazawa, Pathophysiological conditions induced by SARS-CoV-2 infection reduce ACE2 expression in the lung, Front. Immunol. 13 (2022) 1028613.
[52] J. Wang, H. Zhao, Y. An, ACE2 Shedding and the Role in COVID-19, Front. Cell. Infect. Microbiol. 11 (2021) 789180.
[53] T. Yamaguchi, M. Hoshizaki, T. Minato, S. Nirasawa, M.N. Asaka, M. Niiyama, M. Imai, A. Uda, J.F. Chan, S. Takahashi, J. An, A. Saku, R. Nukiwa, D. Utsumi, M. Kiso, A. Yasuhara, V.K. Poon, C.C. Chan, Y. Fujino, S. Motoyama, S. Nagata, J. M. Penninger, H. Kamada, K.Y. Yuen, W. Kamitani, K. Maeda, Y. Kawaoka, Y. Yasutomi, Y. Imai, K. Kuba, ACE2-like carboxypeptidase B38-CAP protects from SARS-CoV-2-induced lung injury, Nat. Commun. 12 (1) (2021) 6791.
[54] R. Ye, Z. Liu, ACE2 exhibits protective effects against LPS-induced acute lung injury in mice by inhibiting the LPS-TLR4 pathway, Exp. Mol. Pathol. 113 (2020) 104350.
[55] Y. Imai, K. Kuba, S. Rao, Y. Huan, F. Guo, B. Guan, P. Yang, R. Sarao, T. Wada, H. Leong-Poi, M.A. Crackower, A. Fukamizu, C.C. Hui, L. Hein, S. Uhlig, A. S. Slutsky, C. Jiang, J.M. Penninger, Angiotensin-converting enzyme 2 protects from severe acute lung failure, Nature 436 (7047) (2005) 112–116.
[56] Q. Chen, J. Liu, W. Wang, S. Liu, X. Yang, M. Chen, L. Cheng, J. Lu, T. Guo, F. Huang, Sini decoction ameliorates sepsis-induced acute lung injury via regulating ACE2-Ang (1–7)-Mas axis and inhibiting the MAPK signaling pathway, Biomed. Pharmacother. 115 (2019) 108971.
[57] H. Wang, L. Cong, X. Yin, N. Zhang, M. Zhu, T. Sun, J. Fan, F. Xue, X. Fan, Y. Gong, The Apelin-APJ axis alleviates LPS-induced pulmonary fibrosis and endothelial mesenchymal transformation in mice by promoting Angiotensin-Converting Enzyme 2, Cell. Signal. 98 (2022) 110418.
[58] T.C. Silva de Almeida, K. Lanza, Filha R da Silva, L.M.C. C Campos, E.G. Fonseca, M.W. Chagas, N.P. Rocha, M.A. de Sá, M.A.R. Vieira, M.V. Caliari, L.M. Kangussu, A.J. Ferreira, E. Simões, A.C. Silva, ACE2 activator diminazene aceturate exerts renoprotective effects in gentamicin-induced acute renal injury in rats, Clin. Sci. (Lond) 134 (23) (2020) 3093–3106.
[59] C. Zhang, X. Cao, H. Wang, Z. Li, Y. Zhang, The ACE2 activator diminazene aceturate ameliorates colitis by repairing the gut-vascular barrier in mice, Microvasc. Res. 148 (2023) 104544.
[60] E. Velkoska, S.K. Patel, L.M. Burrell, Angiotensin converting enzyme 2 and diminazene: role in cardiovascular and blood pressure regulation, Curr. Opin. Nephrol. Hypertens. 25 (5) (2016) 384–395.
[61] T. Qaradakhi, L.K. Gadanec, K.R. McSweeney, A. Tacey, V. Apostolopoulos, I. Levinger, K. Rimarova, E.E. Egom, L. Rodrigo, P. Kruzliak, P. Kubatka, A. Zulli, The potential actions of angiotensin-converting enzyme II (ACE2) activator diminazene aceturate (DIZE) in various diseases, Clin. Exp. Pharmacol. Physiol. 47 (5) (2020) 751–758.
[62] X. Lin, W. Lin, Y. Zhuang, F. Gao, Angiotensin-Converting Enzyme 2 Inhibits Lipopolysaccharide-Caused Lung Fibrosis via Downregulating the Transforming Growth Factor beta-1/Smad2/Smad3 Pathway, J. Pharmacol. Exp. Ther. 381 (3) (2022) 236–246.
[63] L.F. Wang, Y.Y. Sun, Q. Pan, Y.Q. Yin, X.M. Tian, Y. Liu, T. Bu, Q. Zhang, Y. A. Wang, J. Zhao, Y. Luo, Diminazen Aceturate Protects Pulmonary Ischemia-Reperfusion Injury via Inhibition of ADAM17-Mediated Angiotensin-Converting Enzyme 2 Shedding, Front. Pharmacol. 12 (2021) 713632.
[64] S. Joshi, N. Balasubramanian, G. Vasam, Y.P. Jarajapu, Angiotensin converting enzyme versus angiotensin converting enzyme-2 selectivity of MLN-4760 and DX600 in human and murine bone marrow-derived cells, Eur. J. Pharmacol. 774 (2016) 25–33.
[65] M. Li, Y. Wang, M. Li, X. Wu, S. Setrerrahmane, H. Xu, Integrins as attractive targets for cancer therapeutics, Acta Pharm. Sin. B 11 (9) (2021) 2726–2737.
[66] P. Tomakidi, S. Schulz, S. Proksch, W. Weber, T. Steinberg, Focal adhesion kinase (FAK) perspectives in mechanobiology: implications for cell behaviour, Cell Tissue Res. 357 (3) (2014) 515–526.
[67] H.K. Avraham, T.H. Lee, Y. Koh, T.A. Kim, S. Jiang, M. Sussman, A.M. Samarel, S. Avraham, Vascular endothelial growth factor regulates focal adhesion assembly in human brain microvascular endothelial cells through activation of the focal adhesion kinase and related adhesion focal tyrosine kinase, J. Biol. Chem. 278 (38) (2003) 36661–36668.

[68] J.Y. Park, H.M. Park, S. Kim, K.B. Jeon, C.M. Lim, J.T. Hong, D.Y. Yoon, Human IL-32thetaA94V mutant attenuates monocyte-endothelial adhesion by suppressing the expression of ICAM-1 and VCAM-1 via binding to cell surface receptor integrin alphaVbeta3 and alphaVbeta6 in TNF-alpha-stimulated HUVECs, Front. Immunol. 14 (2023) 1160301.
[69] N. Amruta, G. Bix, ATN-161 Ameliorates Ischemia/Reperfusion-induced Oxidative Stress, Fibro-inflammation, Mitochondrial damage, and Apoptosis-mediated Tight Junction Disruption in bEnd. 3 Cells, Inflammation 44 (6) (2021) 2377–2394.
[70] V. Tiwari, J. Singh, P. Tiwari, S. Chaturvedi, S. Gupta, A. Mishra, S. Singh, M. Wahajuddin, K. Hanif, S. Shukla, ACE2/ANG-(1–7)/Mas receptor axis activation prevents inflammation and improves cognitive functions in streptozotocin induced rat model of Alzheimer's disease-like phenotypes, Eur. J. Pharmacol. 946 (2023) 175623.
[71] J.C. Dawson, A. Serrels, D.G. Stupack, D.D. Schlaepfer, M.C. Frame, Targeting FAK in anticancer combination therapies, Nat. Rev. Cancer 21 (5) (2021) 313–324.
[72] X. Chen, Y. Zhao, X. Wang, Y. Lin, W. Zhao, D. Wu, J. Pan, W. Luo, Y. Wang, G. Liang, FAK mediates LPS-induced inflammatory lung injury through interacting TAK1 and activating TAK1-NFkappaB pathway, Cell Death Dis. 13 (7) (2022) 589.
[73] C. Li, Y. Liu, Y. Li, R. Tai, Z. Sun, Q. Wu, Y. Liu, C. Sun, Collagen XV Promotes ER Stress-Induced Inflammation through Activating Integrin beta1/FAK Signaling Pathway and M1 Macrophage Polarization in Adipose Tissue, Int. J. Mol. Sci. 22 (18) (2021).
[74] L.Y. Romanova, J.F. Mushinski, Central role of paxillin phosphorylation in regulation of LFA-1 integrins activity and lymphocyte migration, Cell Adh. Migr. 5 (6) (2011) 457–462.